

Mapping the lifetimes of local opening events in a native state protein

BIRTHE B. KRAGELUND,¹ BO HEINEMANN,^{1,3} JENS KNUDSEN,²
AND FLEMMING M. POULSEN¹

¹Carlsberg Laboratorium, Kemisk Afdeling, Gamle Carlsberg Vej 10, DK-2500 Valby, Copenhagen, Denmark

²Institute of Biochemistry, Odense University, Campusvej 55, DK-5230 Odense M, Denmark

(RECEIVED April 7, 1998; ACCEPTED June 26, 1998)

Abstract

The rate constants for the processes that lead to local opening and closing of the structures around hydrogen bonds in native proteins have been determined for most of the secondary structure hydrogen bonds in the four-helix protein acyl coenzyme A binding protein. In an analysis that combines these results with the energies of activation of the opening processes and the stability of the local structures, three groups of residues in the protein structure have been identified. In one group, the structures around the hydrogen bonds have frequent openings, every 600 to 1,500 s, and long lifetimes in the open state, around 1 s. In another group of local structures, the local opening is a very rare event that takes place only every 15 to 60 h. For these the lifetime in the open state is also around 1 s. The majority of local structures have lifetimes between 2,000 and 20,000 s and relatively short lifetimes of the open state in the range between 30 and 400 ms. Mapping of these groups of amides to the tertiary structure shows that the openings of the local structures are not cooperative at native conditions, and they rarely if ever lead to global unfolding. The results suggest a mechanism of hydrogen exchange by progressive local openings.

Keywords: ACBP; hydrogen exchange; NMR; protein dynamics; two-state folding

The hydrogen exchange reactions of amides in native state globular proteins are a result of dynamic processes. These processes may be the origin of local and global protein stability and of protein folding and unfolding (Kim et al., 1993; Kim & Woodward, 1993; Mayo & Baldwin, 1993; Bai et al., 1995; Clarke & Fersht, 1996). Determination of the kinetics and a further characterization of the events preceding hydrogen exchange may therefore contribute to the understanding of these very important protein properties.

The kinetics of the processes that lead to hydrogen bond opening and hydrogen exchange in proteins has a complex but well understood influence on the kinetics of the measurable hydrogen exchange process (Hvidt & Nielsen, 1966). Therefore, the rate constants of opening and closing can be obtained from hydrogen exchange kinetics (Roder et al., 1985; Pedersen et al., 1993; Arington & Robertson, 1997). A method is described that determines the rate constants of the local opening processes in a native state

protein. The validity of the method is being demonstrated for a number of secondary structure amides in one globular protein, the four α -helix bundle acyl-coenzyme A binding protein, ACBP (Mikkelsen et al., 1987; Andersen & Poulsen, 1993, 1994). The rate constants of segmental opening and closing provide a timetable for the lifetimes of local opening events occurring in the native state protein, and they permit mapping of the events that lead to opening of both exterior and interior hydrogen bonds in the protein. The set of lifetimes provides a description of the scenario of dynamic events in the native protein and their potential role in global folding and unfolding of the protein.

Hydrogen exchange

In a protein an amide hydrogen can be protected from reactions with solvent either by a persistent hydrogen bond, or because it is buried in the interior of the protein. Structural fluctuations are therefore required to break the hydrogen bond and/or to expose the amide to exchange. Many models describing the protein dynamics that lead to hydrogen exchange in folded proteins have been proposed. These have all been described extensively in several reviews including the breathing model, the penetration model, the mobile defect model, the local unfolding model, and the global unfolding model (Hvidt & Nielsen, 1966; Englander et al., 1972; Englander, 1975; Richards, 1979; Wagner & Wüthrich, 1979; Wood-

Reprint requests to: Flemming M. Poulsen, Carlsberg Laboratorium, Kemisk Afdeling, Gamle Carlsberg Vej 10, Copenhagen DK-2500 Valby, Denmark; e-mail: fmp@crc.dk.

³Present address: Universität Mainz, Inst. f. Allgemeine Botanik, Müllerweg 6, D-55099 Mainz, Germany.

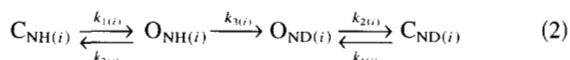
Abbreviations: ACBP, acyl-coenzyme A binding protein; ESI-MS, electrospray ionization mass spectrometry; NMR, nuclear magnetic resonance; HSQC, heteronuclear single quantum coherence; ppm, parts per million.

ward & Hilton, 1979; Barksdale & Rosenberg, 1982; Wagner, 1982; Woodward et al., 1982).

Independent of mechanism, the hydrogen exchange reaction between protein amide hydrogen and solvent water hydrogen can be described by the common model of a two-step reaction scheme (Linderstrøm-Lang, 1955; Hvistendahl & Nielsen, 1966). In this model the first step is a reversible first order reaction,



where $C_{NH(i)}$ is the closed peptide segment (i) and $O_{NH(i)}$ is the exchange active peptide segment (i). $k_1(i)$ is the rate constant for the opening process and $k_2(i)$ is the rate constant for the closing process. In water the exchange active state $O_{NH(i)}$ can exchange its amide hydrogen in a chemical exchange reaction with a hydrogen of water. However, this process cannot be observed directly. To measure this process, the reaction can be studied in deuterium oxide and the replacement of the amide hydrogen with the solvent deuterium can be recorded by techniques such as nuclear magnetic resonance spectroscopy (NMR) and mass spectrometry. The reaction scheme is then



where in $O_{ND(i)}$ the hydrogen has been exchanged with deuterium. The second step of Equation 2 is the bimolecular chemical exchange process, which in practice is a pseudo first order reaction and $k_3(i)$ is the rate constant. The exchange reaction of an amide hydrogen can take place in a reaction directly with water or it can be catalyzed by acid (hydroxonium ions) or base (hydroxide ions) (Gregory et al., 1983; Perrin, 1989), such that the observed exchange rate $k_o(i)$ is the sum of contributions from each of these three reactions.

The model

The time-dependent decays of $[C_{NH(i)}]$ and $[O_{NH(i)}]$ are two exponential functions, representing each of the two consecutive first order reactions. In practice, for protein amide exchange, only the exponential term of the decay of $[C_{NH(i)}]$ can be observed. This is because the initial concentration of $O_{NH(i)}$ at native conditions is small, and the rate constant $k_3(i)$ so large, that within the typical dead time of the exchange experiment, this contribution has vanished. Therefore, assuming first order kinetics and neglecting rehydrogenation in a hydrogen to deuterium exchange situation, the observed exchange rate, $k_o(i)$, for one amide segment (i) is given by (Frost & Pearson, 1953; Hvistendahl, 1964, 1973):

$$k_o(i) = \frac{1}{2} (k_1(i) + k_2(i) + k_3(i)) - ((k_1(i) + k_2(i) + k_3(i))^2 - 4k_1(i)k_3(i))^{1/2}. \quad (3)$$

Provided $k_1(i)$ and $k_2(i)$ are independent of pH $k_3(i)$ is the only pH dependent variable in Equation 3. When the base catalyzed exchange process is dominant, i.e., $k_3(i) = k(i)[OH^-]$, $k_o(i)$ is a function of pH as shown in Figure 1. The first derivative of this function has two limits. At high values of $k_3(i)$, the maximum limit value of $k_o(i)$ is $k_1(i)$. This is the EX1 limit (Frost & Pearson,

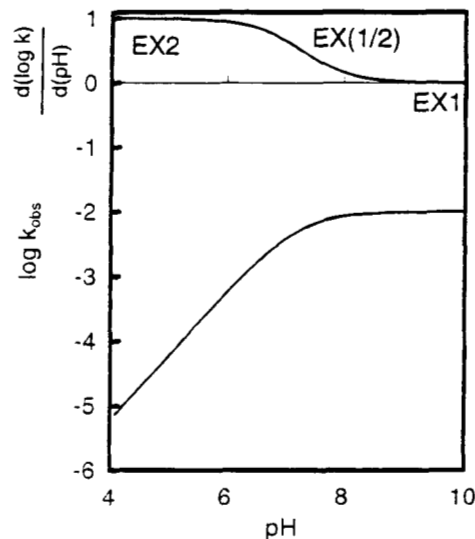


Fig. 1. Simulated pH dependence of k_o for amide exchange according to the full expression Equation 3. Data are simulated in the pH range from pH 4.0 to 10.0 for the situation that only the base catalyzed reaction is active and the rate constants k_1 and k_2 are not pH dependent. The chemical exchange rate $k_3 = 10^8 \times 10^{(pH-14)}$. The three limits of exchange are illustrated in the top panel as the first derivative: EX2 (pH dependence = 1), EX(1/2) ($0 < \text{pH dependence} < 1$), and EX1 (no pH dependence).

1953; Hvistendahl, 1964, 1973; Hvistendahl & Nielsen, 1966) where $\delta(k_o(i))/\delta(k_3(i)) = 0$. At low values of $k_3(i)$, $k_o(i)$ is linearly dependent of $k_3(i)$. This is the EX2 limit (Frost & Pearson, 1953; Hvistendahl, 1964, 1973; Hvistendahl & Nielsen, 1966) where $k_o(i) = (k_1(i)/k_2(i))k_3(i)$ and the slope is $(k_1(i)/k_2(i))$. In the practical logarithmic presentation, the slope is 1 and $(k_1(i)/k_2(i))$ is the value of the function at $\log k_3(i) = 0$.

The residue dependent variations of $k_1(i)$, $k_2(i)$, and $k_3(i)$ shift the value for the observed rate constant, $\log k_o(i)$ in Figure 1, by a simple transposition where increasing $k_1(i)$ and/or $k_3(i)$ shift $k_o(i)$ to higher values, and increasing $k_2(i)$ shifts $k_o(i)$ to a higher maximum with higher $k_3(i)$ values.

In the range between the two boundary conditions, the simplifications of the full rate expression used in the EX1 and EX2 limits are not applicable. This range, which has often been ignored, is here referred to as the EX(1/2) range. When the rate constants $k_1(i)$ and $k_2(i)$ are not themselves pH dependent, amides exchanging in the EX(1/2) range can easily be distinguished from amides in the EX1 and the EX2 range by the slope $\alpha_{pH} = \Delta \log k_o(i)/\Delta pH$ of the pH dependence of the hydrogen exchange kinetics. For EX2 amides $\alpha_{pH} = 1$, for EX1 amides $\alpha_{pH} = 0$, and for EX(1/2) amides α_{pH} is between 0 and 1 (Fig. 1). For amides with exchange kinetics in the EX(1/2) range, there is a unique possibility to determine the rate constants $k_1(i)$ and $k_2(i)$ simply by nonlinear fitting to the pH dependence of the exchange kinetics using the full expression for $k_o(i)$ (Equation 3).

A nonlinear three-parameter fit analysis of Equation 3 to a data set with a sufficient number of experimental data points can in principle determine all three parameters, $k_1(i)$, $k_2(i)$, and $k_3(i)$. The only assumption made for this calculation is the reaction scheme (Equation 2). It is shown here that $k_1(i)$ can be obtained unambiguously from this analysis whereas $k_2(i)$ and $k_3(i)$ are too strongly correlated to be determined.

If it is assumed that a site specific random coil rate constant (Bai et al., 1993) can be applied as $k_3(i)$, the experimental data for a given residue can be fitted in a two-step one-parameter fit, where $k_1(i)$ is obtained initially from the three-parameter fit, and subsequently $k_1(i)$ and $k_3(i)$ are used to determine $k_2(i)$. Previously, it has been described how $k_1(i)$ and $k_2(i)$ can be determined in a two-parameter fit where it is assumed that $k_3(i)$ is known (Roder et al., 1985; Pedersen et al., 1993; Arrington & Robertson, 1997).

In the present work, the pH dependence of the observed hydrogen exchange rates of individual amides by NMR has been used to determine the two rate constants $k_1(i)$ and $k_2(i)$ for the amides in the four-helix protein ACBP. In a combination of both the nonlinear three-parameter approach and the one-parameter fit, measures of the lifetimes of the local opening events leading to hydrogen exchange have been obtained.

Acyl coenzyme A binding protein (ACBP)

The 86 residue, four- α -helix bundle protein ACBP has previously been proven to be a good model protein for studies of protein dynamics and folding. ACBP has the advantages that it contains mainly one type of secondary structure, the α -helix, it is a single-domain protein, it has no cystine bridges, and it refolds reversibly (Kragelund et al., 1993, 1995b). The dynamic properties of ACBP in the liganded and in the nonliganded forms have been examined by ^{15}N -relaxation studies and similarly the perturbation by ligand binding of amide hydrogen exchange has been studied (Rischel et al., 1994; Kragelund et al., 1995a). The global processes of folding and unfolding of ACBP have been characterized in detail as observed by stopped-flow techniques combined with, respectively, fluorescence, far- and near-UV circular dichroism and by deuterium pulse labeling in combination with electrospray ionization mass spectrometry (ESI-MS) (Kragelund et al., 1995b).

Results

Identification of EX(1/2) amides

When the rate constants $k_1(i)$ and $k_2(i)$ are themselves pH dependent, the method of determining these from the pH dependence of the amide hydrogen exchange kinetics is clearly not applicable. It is therefore important to distinguish between hydrogen bond amides for which the two rate constants are not affected by pH from those which are.

The ratio $k_1(i)/k_2(i)$ is the equilibrium constant for the local opening event and is thus a measure for the stability of the closed form of the residue (i). A pH-induced change of stability is a result of changes in local electrostatic properties. These can be monitored by the pH dependence of the exchange kinetics, α_{pH} . For an EX2 amide which experiences no pH induced change in stability, $\alpha_{\text{pH}} = 1$. In ACBP this is the situation readily recognized for three amides with $\alpha_{\text{pH}} = 1$ (A9, T35, E79).

For a typical EX2-amide, the observed exchange rates increase with pH. If the stability is also increasing with pH, amide exchange rates will increase by less than one per unit of pH ($\alpha_{\text{pH}} < 1$). If the stability decreases with pH, the increase will be larger than 1 ($\alpha_{\text{pH}} > 1$). For an EX1 amide the exchange is independent of pH, but if stability increases with pH, α_{pH} will be negative, and if stability decreases, $\alpha_{\text{pH}} > 0$. An amide that has $\alpha_{\text{pH}} < 1$ is therefore either an EX2 amide whose environment is stabilizing with

increasing pH, an EX1 amide that is destabilizing with increasing pH, or an amide that exchanges in the EX(1/2) range. The three possible scenarios are not immediately distinguishable.

For the majority (25) of the slowly exchanging amides in ACBP, α_{pH} is less than 1 in the pH range between 5.2 and 7.4 (Table 1). This means that for each individual amide in this group, it is necessary to distinguish whether the amide is in a structural environment that is stabilizing with increasing pH or the stability of the amide is unaffected by pH, resulting in exchange kinetics in the EX(1/2) range. For a few amides α_{pH} is significantly larger than 1 in the range of pH above 7.4. The exchange of these amides shows the onset of a common destabilization of ACBP at pH above 7.4. For this reason the present analysis has been restricted to the pH range of 5.2 to 7.4.

Using the pH dependence of chemical shifts and the pH dependence of hydrogen exchange to identify pH dependent stability effects

Independent studies of the global stability of ACBP by guanidinium chloride denaturation show that the protein is stable in the pH range between pH 5 and pH 7.4 ($\Delta G_{\text{U-F}} = 5.6 \pm 0.4 \text{ kcal mol}^{-1}$). However, one of the most sensitive parameters to electrostatic and structural changes is the chemical shift of an NMR resonance line. By recording the pH dependence of the chemical shifts of the amide atoms, local pH-induced perturbations of the native structure can be identified. For ACBP in the pH range of 5.2 to 7.4, the majority of the amides show very small pH dependent ^1H and ^{15}N chemical shift changes, respectively, less than 0.05 ppm and less than 0.5 ppm. This is unambiguous evidence that there are no significant pH induced local conformational changes, and also that there are no significant changes in the local electrostatic environment. There are, however, a few amides with large changes in chemical shift with pH. In helix A2 the deprotonation of H30 ($\text{p}K_a = 7.5$) with increasing pH results in relatively large chemical shift changes (for ^1H , 0.04–0.15 ppm; for ^{15}N , 0.5–2.5 ppm) of the amides of H30, Y31, K32, Q33, A34, and T64. Apart from H30, which has a ^1H chemical shift change of 0.06 and an ^{15}N chemical shift change of 1.30 ppm, the largest perturbations are seen for A34 and T64 with ^1H and ^{15}N chemical shifts changes of (0.15, 0.55 ppm) and (0.05, 1.0 ppm), respectively. T64 is close to H30 (approximately 8 Å).

In summary the only electrostatic perturbation that is observable in the pH range considered originates from the deprotonation of H30. This has neither a significant effect on the local nor on the global stability as measured by guanidine hydrochloride titrations at various pH values (data not shown). For all the other amides in this study, there are no significant changes of the local electrostatic environment in the pH range concerned. The pH dependence of hydrogen exchange kinetics with $\alpha_{\text{pH}} < 1$ that has been observed for a large number of amides in ACBP can therefore be assigned here to the interim region of EX1 and EX2, the EX(1/2) region. For these amides it is possible to determine $k_1(i)$ and $k_2(i)$ as described above. The two alternative scenarios for the reduced pH dependence can both be disregarded.

The intrinsic chemical exchange rate, $k_3(i)$

For the determination of $k_2(i)$, an additional provision is that the residue specific intrinsic rate constants $k_3(i)$ (Bai et al., 1993) are applicable. This implies that only nearest neighbor side-chain in-

Table 1. Lifetimes of C and O from amide hydrogen exchange in ACBP^a

Residue	Lifetime C ^a ($\times 10^{-3}$)(1/ k_1) (s)	Lifetime O ^a (1/ k_2) (s)	ΔG_{HX} (kcal mol ⁻¹)	$E_{a,\text{HX}}$ (kcal mol ⁻¹)	$\Delta \log(k_o)/\Delta \text{pH}$	$\Delta \delta/\Delta \text{pH}$ (¹ H, ¹⁵ N) (ppm)
A8	0.27 ± 0.10	0.08 ± 0.03	4.84 ± 0.33	24.7 ± 0.6	0.93 ± 0.03	0.02,0.05
A9	—	—	4.92 ± 0.03	—	1.02 ± 0.03	0.01,0.16
E10	1.06 ± 0.04	0.72 ± 0.03	4.34 ± 0.03	19.5 ± 0.7	0.79 ± 0.03	0.01,0.05
V12	0.98 ± 0.37	1.32 ± 0.58	3.93 ± 0.34	17.4 ± 0.8	0.82 ± 0.02	0.03,0.30
S29	2.87 ± 0.99	0.037 ± 0.014	6.70 ± 0.31	25.9 ± 0.6	0.85 ± 0.02	0.01,0.15
H30	4.60 ± 1.09	0.12 ± 0.03	6.28 ± 0.22	19.9 ± 1.0	0.49 ± 0.07	0.06,1.30
Y31 ^{b,c}	133 ± 19	0.84 ± 0.32	7.12 ± 0.24	64.8 ± 1.7	0.35 ± 0.01	0.08,0.60
K32 ^c	64.2 ± 8.1	0.94 ± 0.23	6.62 ± 0.17	29.3 ± 5.0	0.51 ± 0.03	0.04,0.07
A34 ^c	18.3 ± 1.9	0.11 ± 0.03	7.17 ± 0.17	48.3 ± 7.6	0.78 ± 0.09	0.15,0.55
T35	—	—	7.72 ± 0.02	—	1.07 ± 0.09	0.01,0.03
G37	1.39 ± 0.46	0.029 ± 0.010	6.41 ± 0.29	33.7 ± 0.4	0.89 ± 0.03	0.03,0.60
W55	(0.58 ± 0.24)	(0.50 ± 0.22)	4.19 ± 0.36	22.2 ± 4.2	0.92 ± 0.04	0.03,0.50
D56	0.85 ± 0.31	0.10 ± 0.04	5.38 ± 0.32	40.5 ± 0.8	0.89 ± 0.04	0.02,0.25
A57	1.99 ± 0.56	0.074 ± 0.023	6.06 ± 0.25	—	0.95 ± 0.05	0.03,0.40
W58 ^c	9.95 ± 1.89	0.19 ± 0.05	6.47 ± 0.19	53.5 ± 5.6	0.86 ± 0.07	0.04,0.40
N59	8.93 ± 2.63	0.059 ± 0.023	7.09 ± 0.29	49.2 ± 1.2	0.94 ± 0.09	0.04,0.20
E60	4.19 ± 1.21	0.045 ± 0.015	6.80 ± 0.26	43.2 ± 0.7	0.91 ± 0.09	0.02,0.60
K62	6.32 ± 0.92	0.36 ± 0.06	5.81 ± 0.13	16.4 ± 2.6	0.79 ± 0.04	0.04,0.35
G63	1.68 ± 0.25	0.96 ± 0.19	4.44 ± 0.15	13.9 ± 1.9	0.56 ± 0.03	0.02,0.10
T64	3.58 ± 0.94	0.059 ± 0.019	6.55 ± 0.25	31.9 ± 0.6	0.80 ± 0.06	0.02,1.00
M70 ^c	47.4 ± 7.4	0.14 ± 0.04	7.55 ± 0.20	35.1 ± 0.7	0.65 ± 0.02	0.01,0.40
A72	11.6 ± 0.3	0.28 ± 0.01	6.32 ± 0.03	20.0 ± 0.2	0.54 ± 0.04	0.00,0.80
I74 ^{b,c}	159 ± 28	2.59 ± 1.18	6.56 ± 0.29	35.8 ± 3.4	0.51 ± 0.04	0.01,0.30
E78 ^{b,c}	226 ± 30	12.7 ± 4.9	5.82 ± 0.24	—	0.34 ± 0.03	0.02,0.10
E79	(11.8 ± 2.8)	(0.085 ± 0.024)	7.06 ± 0.22	—	1.02 ± 0.11	0.02,0.40
K81 ^c	67.8 ± 18.5	0.23 ± 0.12	7.43 ± 0.35	—	0.55 ± 0.03	0.01,0.30
K82	4.09 ± 0.34	0.37 ± 0.04	5.54 ± 0.09	14.4 ± 0.30	0.66 ± 0.03	0.01,0.40
Y84	0.90 ± 0.37	0.71 ± 0.36	4.25 ± 0.39	9.6 ± 1.6	0.77 ± 0.04	0.01,0.05

^aNumbers in parentheses are fitted better to an EX2 exchange limit: C, closed state; O, open state. The calculations of the standard deviations include the standard deviations of the individual rate constants $k_o(i)$. The standard deviations of the latter also include the standard deviations of the peak integrals used to determine $k_o(i)$. Standard deviations of ΔG_{HX} includes standard deviations of both $k_1(i)$ and $k_2(i)$.

^bAmides with exchange close to the EX1 exchange limit

^cAmides with two distinct exchange decays. Also the amides of Q33, I39, L61, and V77 had two distinct exchange decays, but for these amides either too few data point were acquired or exchange was only measured at high pH.

ductive effects are active, and therefore, that the exchanging amide hydrogen must be fully exposed to solvent in order to exchange. The rate constants $k_1(i)$ and $k_2(i)$ are for the processes that, respectively, bring the molecule from the native and fully folded form to the fully exposed amide and back. It is possible that in this process there could be stable partly opened intermediates. From these forms amide hydrogen exchange may also occur. It is difficult to eliminate this possibility, however, the best indication that the k_3 assumption is valid is seen for the amides close to the EX2 limit. Here identical $k_1(i)/k_2(i)$ are determined by the two independent methods: From the pH dependence the ratio is measured independent of $k_3(i)$, and from the nonlinear fitting procedures where the intrinsic rate constant $k_3(i)$ is used to determine $k_2(i)$.

The pH and temperature dependence of hydrogen exchange in ACBP

All of the 56 examined amides in ACBP show a pH-dependent amide hydrogen exchange reaction. The cross peak intensities fitted to Lorentzian line shapes are shown for several pH values for

A72 (see Fig. 2). The pH-dependent variations in the observed exchange rates are shown for nine amides in Figure 3. For 45 amides the exchange could be recorded at three or more of the eight pH values for which exchange was measured. The exchange of some of these amides was either affected at high pH or was measurable only at pH values above 7.4. As a result 28 amides were considered for determination of $k_1(i)$ and $k_2(i)$ (Fig. 4; Table 1). These amides were grouped according to their pH dependence into an EX(1/2) and an EX2 group. For 25 individual amides (i) in the EX(1/2) group, the opening rate constants $k_1(i)$ were determined using the nonlinear three-parameter fitting method. The fastest opening reactions occur with a rate of $3 \times 10^{-3} \text{ s}^{-1}$ and the slowest with rates less than 10^{-5} s^{-1} (see Table 1). Subsequently, the rate constants of local closing, $k_2(i)$, were determined to range from the slowest of 0.1 s^{-1} to the fastest of 35 s^{-1} (Table 1). Among the sites with the longest lifetimes in the open form, there is one distinct category represented by the shortest observed lifetimes in the closed form (A8, E10, V12, W55, D56, G63, Y84) (Fig. 5). There are four sites with a very long lifetime in the closed form (Y31, K32, I74, E78). These have closing rates

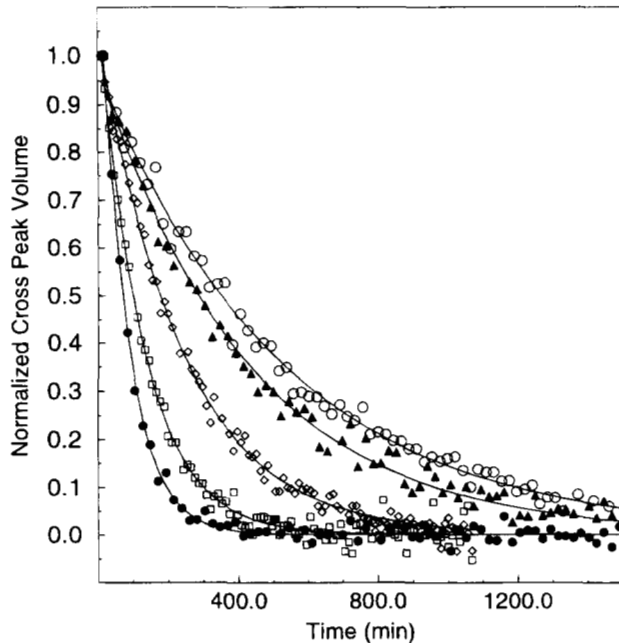


Fig. 2. Hydrogen exchange of Ala72. Hydrogen to deuterium exchange decay curves by HSQC cross peak intensities of the amide hydrogen of Ala72 in ACBP at different pH values. (\circ) pH 8.07, (\blacklozenge) pH 7.40, (\square) pH 6.91, (\bullet) pH 6.65, and (*) pH 6.12. Each point represents the cross peak volume from one HSQC spectrum and solid lines are best single exponential fits. Only exchange below pH 7.4 were used for determination of $k_1(A72)$ and $k_2(A72)$.

ranging from 10^{-1} to 10 s^{-1} (Fig. 5). A third and largest group of amides have closing rates around 10 s^{-1} with opening rates from 10^{-2} to 10^{-4} s^{-1} (Fig. 5).

From the ratio of $k_1(i)/k_2(i)$, the difference in free energy of the individual open and closed equilibrium states could be determined as $\Delta G_{\text{HX}}(i) = (RT \ln(k_1(i)/k_2(i)))$ (Fig. 4; Table 1). For amides in the EX2 group, the ratio $k_1(i)/k_2(i)$ was determined directly from the pH dependence of the hydrogen exchange rate. The free energy differences were measured for the amides to range between 4 and 7 kcal mol $^{-1}$.

From the temperature dependence of the observed exchange rates as seen in Figure 3, the energies of activation for exchange $E_{a,\text{HX}}(i)$ were determined for 31 amides using an Arrhenius analysis (Fig. 6). The measured energies of activation range from 10 to 65 kcal mol $^{-1}$ (Table 1).

Hydrogen exchange by alternative pathways of opening

For several amides, the hydrogen exchange kinetics was seen to decay from both a fast and a slow component (Fig. 7; Table 1). This indicates that the individual amide may exchange either by two (or more) mechanisms of opening, or that the native state exists in two discrete conformations in slow exchange equilibrium with each other. In all cases it was found that the most abundant component had the slowest exchange kinetics, and in all cases this is the process reported here. We exclude these observations to origin from the 5% of the protein sample with the N-terminal acetylated since the amides with two exchange decays are not close to the site of acetylation. The present study does not permit

a distinction of the possible pathways that the two-component kinetic decays suggest.

Discussion

The lifetime of the closed hydrogen bond sites and mapping to structure

The lifetimes of the closed states of the hydrogen bond sites are determined using the nonlinear three-parameter fitting method. These lifetimes are therefore determined without making any assumption regarding the mechanism of the local opening process. The inverse of the measured opening rate constant k_1 is the length of time between two local openings of the structure around a hydrogen bond site (i) leading to an exchange active state. In ACBP the longest lifetime of the closed state measured is more than 200,000 s, the shortest only 270 s. Six amides have very long lifetimes of 50,000 to 200,000 s in the closed form. These are Y31 and K32 in helix A2 and M70, I74, E78, and K81 in helix A4 (Figs. 4, 6). It is common for these sites of hydrogen bonds that each of the two side chains involved has many inter-residue interactions. Also, the hydrogen bonds are in the middle of helices, where the carbonyl of the amide-donor residue and the amide of the carbonyl-acceptor residue each are part of two additional hydrogen bonds. The amide groups and the side chains of Y31 and K32 are directly involved in strong interactions with many hydrophobic residues both in helix A1, helix A3, and in helix A4 (Fig. 8). The four residues in helix A4 are part of the same environment and are interacting with F5, a residue of the hydrophobic minicore at the interface of A1 and A4.

The hydrogen bond sites with shorter lifetimes in the closed form have in common that they are either in the beginning or at the end of helices. Also, it is typical that only one of the two side chains of the hydrogen bond residues is being engaged in side-chain interactions, and only one of the residues may have both the amide and carbonyl groups engaged in a secondary structure hydrogen bond. One such residue is E10 (Fig. 9).

Helix A4 has the largest number of EX(1/2) amides of the four helices. It has four sites, M70, I74, E78, and K81, with extremely long lifetimes. Between these four positions, there are sites with lifetimes 6- to 20-fold shorter. This, together with the large energies of activation for exchange, suggests that in the center of this long helix, there are several sites of high local stability, most likely determined by strong side-chain interactions. The large differences between lifetimes of the closed forms of neighboring amides, which is also seen in the sequence of residues 29–32 of helix A2, suggest that the opening depends on breaking interactions in parts of the structure that are separate from the site of opening and exchange.

The lifetime of the open exchange active hydrogen bond sites and mapping to structure

The lifetimes of the open and exchange active states are $(k_2)^{-1}$. These have been determined here using the rate constant $k_1(i)$ obtained from the nonlinear three-parameter fit and from the assumption that the site specific k_3 is an applicable measure for the chemical exchange reaction. The lifetimes of the locally open states range between 35 ms and up to 10 s.

Four of the amides that rarely ever open (Y31, K32, I74, E78) are also relatively slow to close. This observation suggests that at these sites the interactions keeping the native structure together are

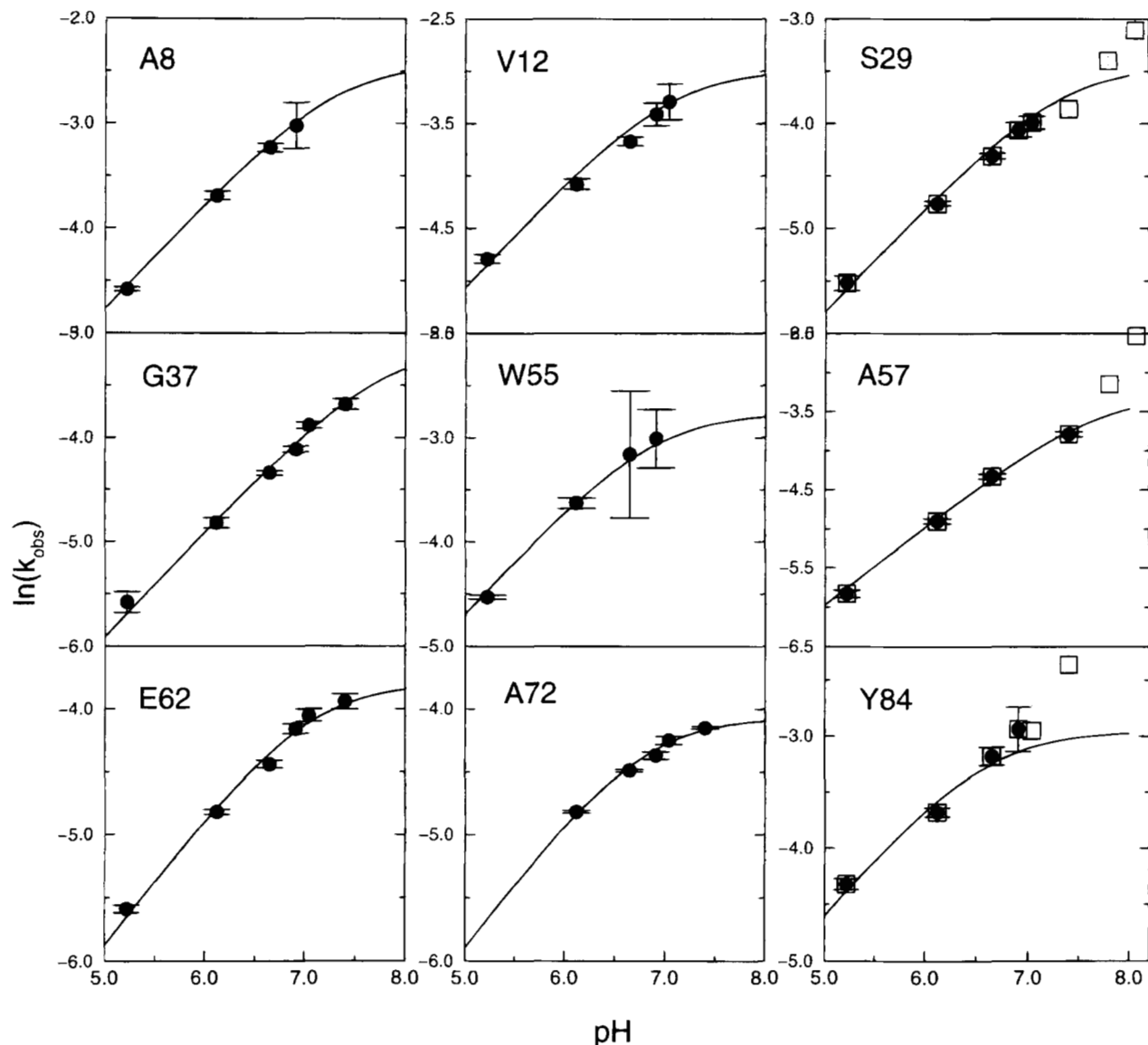


Fig. 3. The pH dependent amide exchange. The pH dependence of the observed exchange rate constants as shown for nine amides. The exchange profiles were fitted by the nonlinear three-parameter fitting procedure and the amides shown represent a wide range of opening and closing rates. The points represented by open squares only at high pH were not included in the fitting of $k_1(i)$ and $k_2(i)$ (see text).

difficult to re-establish when they are broken in a local opening event. Most likely this is because the excursion of the components of the structure to the open form requires larger rearrangements of the native structure.

Several of the frequently open sites are also rapid to close. The short time of opening of these sites suggests that when the hydrogen bond is broken the successful search for the lost partner will be relatively fast. A small group of frequently open sites are slow to close. The sites of this group are likely candidates for the initiation for the more rare and probably more extensive openings.

Progressive local opening

The large dispersion of $k_1(i)$, $k_2(i)$, $\Delta G_{\text{HX}}(i)$, and $E_{\alpha,\text{HX}}(i)$, describing the exchange of amides in ACBP (Fig. 4), shows that the

local opening and local closing processes cannot be a part of a global cooperative unfolding process. The results indicate instead the existence of many local or subglobal cooperative opening processes, a phenomenon described earlier as partial unfolding (PUF) (Bai et al., 1995). The most obvious example is seen in helix A1, where the central six amides are all relatively fast to exchange, and the opening frequencies obtained for three of these, A8, E10, and V12, are similar and some of the highest measured. This helix may open fully once every 1,000 s and the lifetime of this open state could be as long as almost 1.5 s. The obtained rate constants (Table 1) suggest that similar events may take place in the N-terminal of helix A2 and helix A3, the C-terminal of the helix A4 and the type II β -turn structure between A3 and A4. There are no structural indications suggesting that the "frequent" openings occur simultaneously.

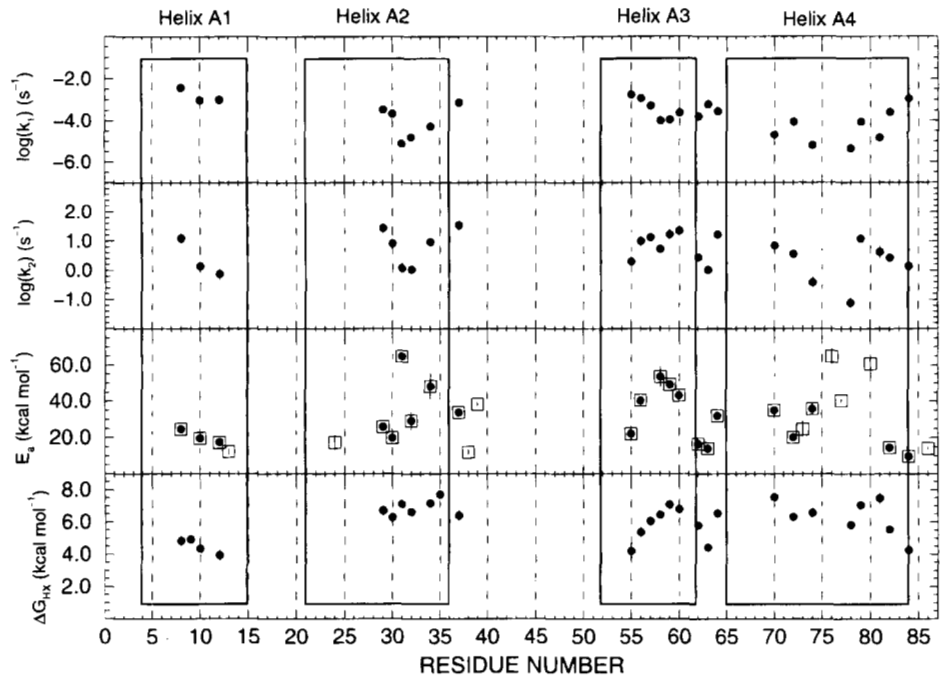


Fig. 4. Sequential variation in the local opening parameters. Four parameters describing the local opening events in ACBP have been determined. In the top panel is shown $\log(k_1)$, in the second panel $\log(k_2)$, in the third panel E_a , and in the bottom panel ΔG_{HX} . Activation energies are shown both as boxes and circles. When only a box is shown, no values for $k_1(i)$ and $k_2(i)$ have been obtained. Boxes indicate the four α -helices of ACBP. Vertical dashed lines for each five residues have been drawn to guide the eye.

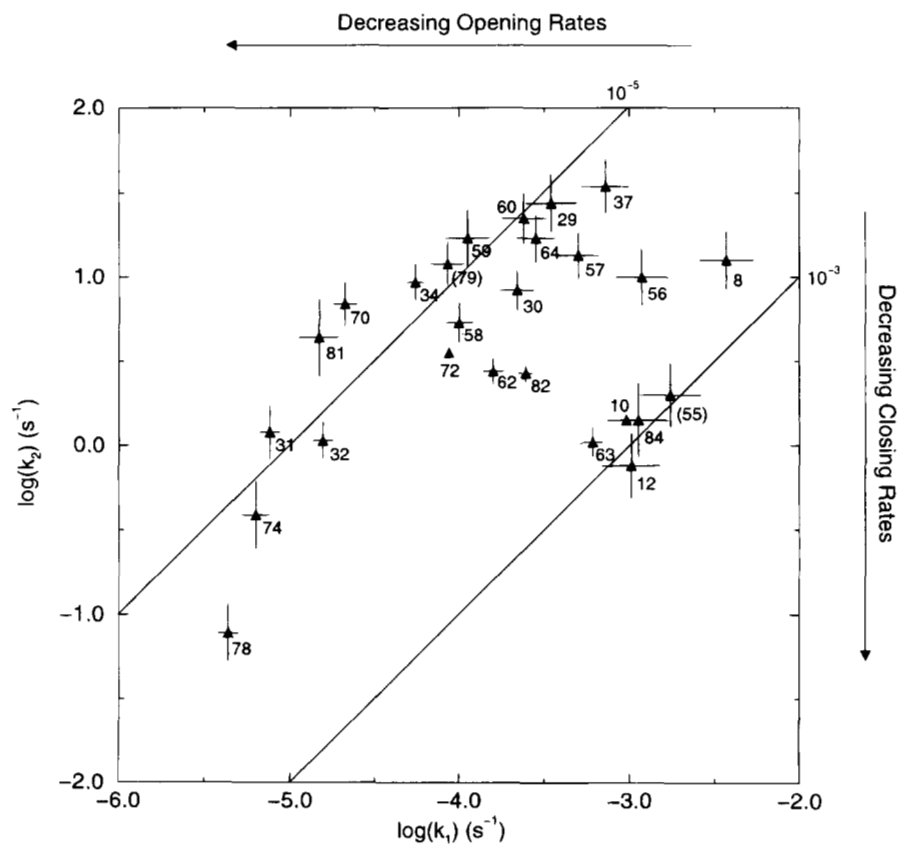


Fig. 5. Distribution of $k_1(i)$ and $k_2(i)$. The distribution of $\log k_1(i)$ and $\log k_2(i)$ for 25 amides in ACBP. Lines at $k_1(i)/k_2(i) = 10^{-5}$ and 10^{-3} are shown to guide the eye and are not intended to represent any correlation. The values for W55 and E79 are shown in parentheses as the exchange is best fitted to an EX2 exchange limit.

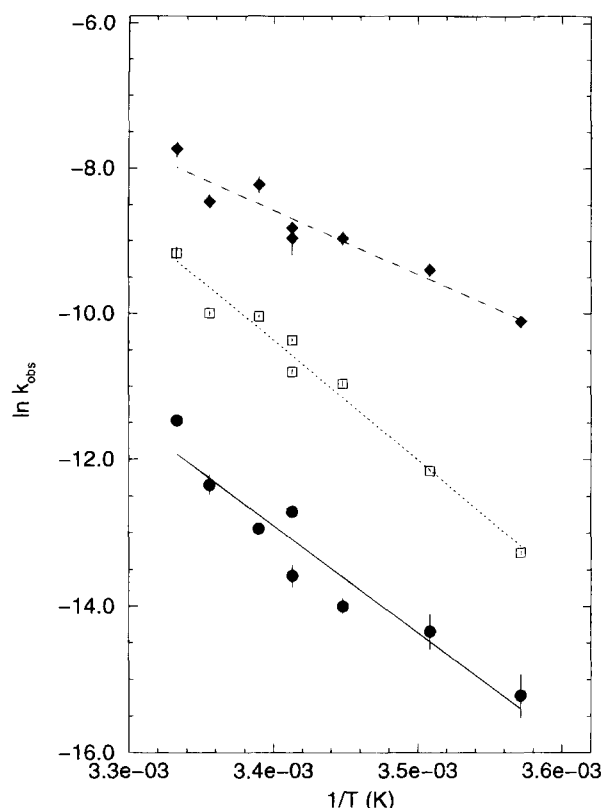


Fig. 6. Arrhenius plot determination of apparent energies of activation for hydrogen exchange in ACBP. The exchange rates as a function of temperature are shown for the amides of (●) Met70, (□) Gly37, and (◆) Val12. All exchange in the EX(1/2) limit but with different energies of activation. A linear fit is shown for each amide and the apparent energy of activation is extracted from the slope of each line.

Hydrogen exchange of a secondary structure amide is the consequence of breaking a hydrogen bond and the subsequent exposure of the exchanging group to solvent. The quantitative measures of the time constants of these events have shown that they are most likely a result of openings both of the side chain and backbone interactions primarily of the two residues involved. Hydrogen exchange kinetics is therefore a measure of the dynamics not only in the peptide backbone. It is more prominently a result of events taking place rather in the body of the structure of a protein than in the peptide backbone, where it is observed. The structural properties at four sites of the hydrogen bond structure might therefore be of relevance for the kinetics of hydrogen exchange reactions. These are the van der Waals' and polar interactions of the two side chains of the secondary structure hydrogen bond and the hydrogen bond formation of, respectively, the carbonyl group and amide group of both residues.

The local openings of helix A1 may occasionally be the triggers of the rare openings of other parts of the structure. The interface of the helices A1 and A4 is maintained by strong hydrophobic interactions between residues of the two helices (Fig. 8). These interactions are destabilized when amides in helix A1 are open. In a fraction of the events where A1 is open, local opening of the hydrogen bonds and amide exchange in the rarely opening hydrogen bonds of A4 may occur. In analogy to this, the most rarely open sites may then open only in a small fraction of the times when both of the other two sets of secondary structures are open.

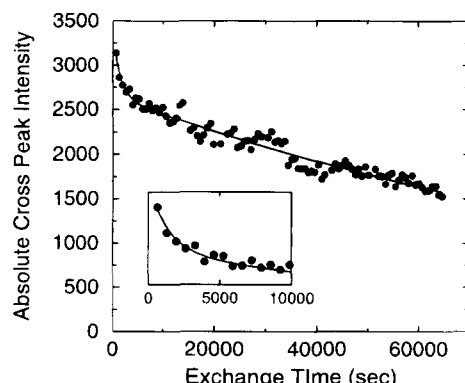


Fig. 7. Double exponential exchange kinetics of K81. Double exponential exchange decays observed for K81. Bold solid line represents the best fit to a sum of two-exponential decays. Insert: Magnification of the initial 10,000 s of amide exchange. The rates and amplitudes are for the fast component $k_{fast} = 7.3 \times 10^{-4} \text{ s}^{-1}$, $A_{fast} = 23.5\%$ and for the slow component applied for k_1 and k_2 determination $k_{slow} = 7.9 \times 10^{-6} \text{ s}^{-1}$, $A_{slow} = 76.5\%$.

The two groups of slowly closing amides (Y31, K32, I74, E78) and (E10, V12, D56, G63, Y84) established by the present results, propose the existence of one type of pathway for hydrogen exchange in folded globular proteins. The local "low energy" and frequent opening in one part of the structure is accompanied by destabilization of associated rare opening regions. In a small fraction of the times the frequently open regions are open, destabilized hydrogen bond sites in the associated regions and the interactions in the structure around them may be exposed.

The path of events leading to hydrogen exchange can be described by a mechanism of progressive local openings (Fig. 10). For each amide there is a probability for exchange when all interactions to each of the two residues implied are either weakened or even broken. For an entire helix the probability of opening then depends on the relaxation of all interactions involved. The exchange of an amide in a particular secondary element will then be less frequent if there are interactions to more than one other secondary element. In ACBP helix A3 is a perfect example of an isolated cooperative local opening event. This helix is interacting only with helix A2. In contrast to helix A1, A2, and A4 by the local opening processes are dependent on simultaneous opening of sites in two or more helices.

Global and local events in other proteins

The dynamics of the local opening events measured by hydrogen exchange kinetics for ACBP can be compared to the dynamics of global unfolding events measured recently in the ovomocid third domain (Arrington & Robertson, 1997). These global opening and closing rates were determined using the method we proposed earlier (Pedersen et al., 1993), but without the three-parameter fitting approach. It was found that in this small protein, which has a very small core, shorter lifetimes of the closed forms ($1/k_1$) as compared to ACBP, but with similar shorter lifetimes of the open forms. This is clearly an expected result from a protein where amides exchange via global opening processes. In contrast, for lysozyme, a protein larger than ACBP and with a larger core, the same picture of local opening events with similar lifetimes as for ACBP was observed (Pedersen et al., 1993).

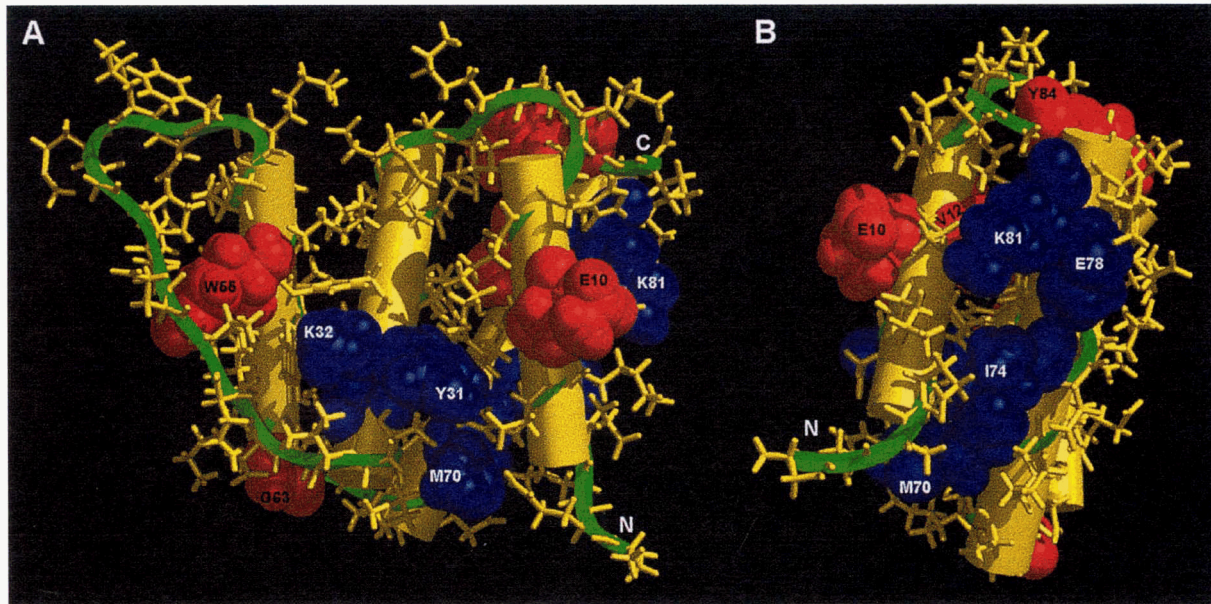


Fig. 8. Core amides, the “rarely open and slow to close.” Amides with long lifetimes of the closed form are shown in blue by space filled g atoms. The core residues are: Y31, K32, M70, I74, V77, E78, and K81. Residues with long lifetimes in the open form, the triggers to progressing local opening, are colored red. These residues are: E10, V12, W55, G63, and Y84. **A:** Front side view of ACBP. **B:** Right side view into the side of helix A4. The four helices are shown in yellow and a ribbon drawn through the backbone atoms is shown in green. The picture was produced by the structure facility of the program PRONTO (Kjær et al., 1994).

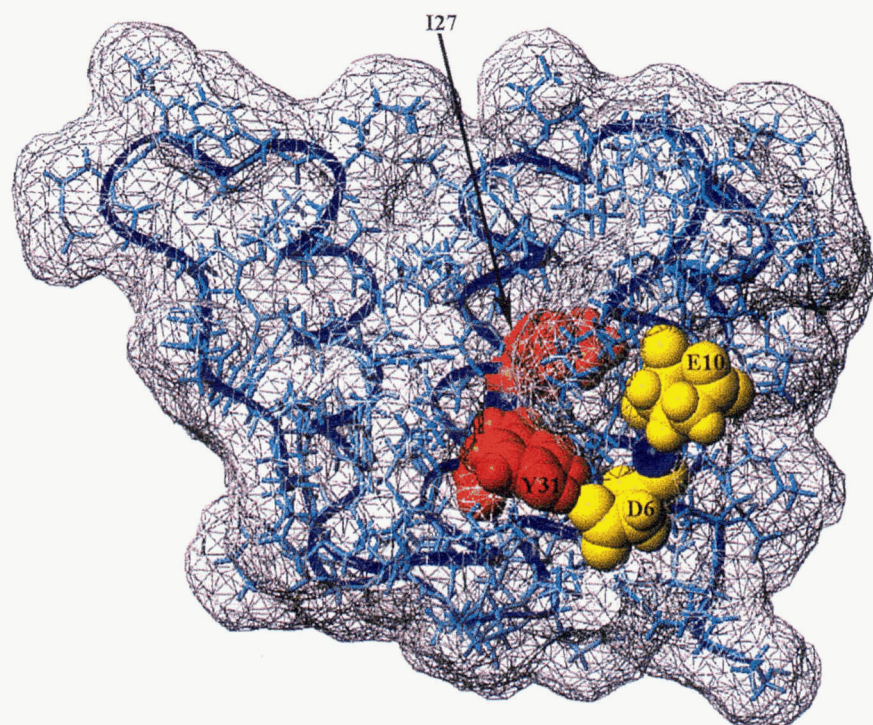


Fig. 9. Structural environment of the two categories of amides. The structural environment around a “rarely open and slow to close” site, the hydrogen bond between I27–Y31 shown in red and the structural environment of a “frequently open and slow to close” site, the hydrogen bond of K6–E10 shown in yellow. The involved residues are shown in space filling atoms. All other residues are shown as surface. The atoms O and H^N of the two hydrogen bonds are colored blue. A smooth ribbon drawn through the C^α atoms is shown in dark blue.

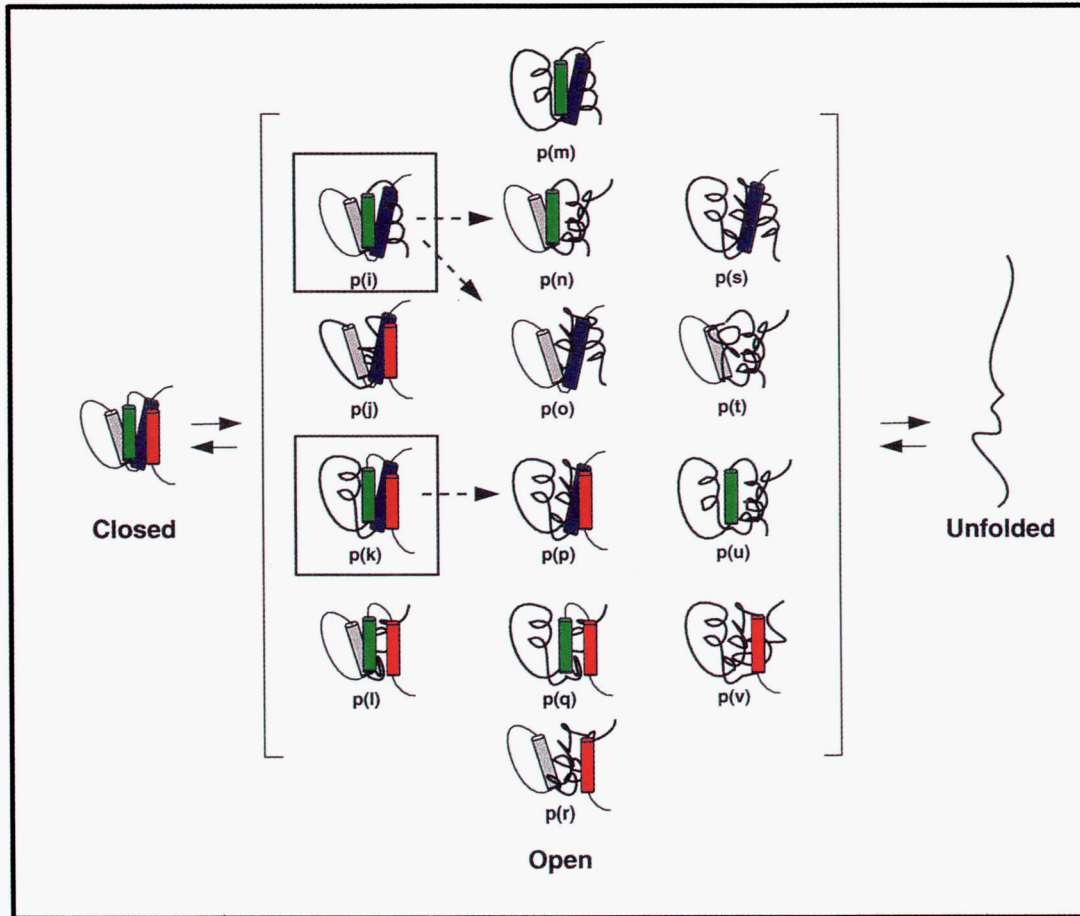


Fig. 10. Progressing local openings. The suggested model of progressing opening is based on the variations of the lifetimes of the open and closed states measured for the individual sites in ACBP. The model proposes that opening of one site will destabilize neighboring sites. Sites that are more frequently open and with long lifetimes in the open state have the highest probabilities of being open. The destabilization effect from these sites on neighboring sites therefore has a higher probability. The diagram presents a schematic model in which opening of one amide in one helix B for simplicity B is shown as an opening of the entire helix. The framed structures have sites with the highest probability of opening. The progressive openings are most likely initiated from these sites as indicated by arrows.

Conclusions

The present study is the first rigorous analysis of the lifetimes of local opening events occurring from a native state protein at non-denaturing condition. The data have been analyzed in a full-expression analysis of the commonly applied two-state exchange reaction.

Three groups of amides were identified: The “fast to close” sites with a wide range of opening frequencies and the “slow to close” sites that are either frequently or rarely open. In the helices of ACBP, locally progressing openings that are initiated from both ends of the helix have been observed. Such openings are more frequent and are associated with looser networks of side chains with fewer contacts. Their closing rates are fast and their excursion of the open structure from the native structure is small. The low-energy, frequently opening sites with slow closing rates observed on the edge of the helices can be occasional triggers of subsequent opening events in the more rarely opening high-energy sites. The dynamics in networks of such high-energy structures with many stabilizing contacts is slow and correlated with larger amplitudes,

higher free energy differences and higher energies of activation. This is a globally progressing opening, which rarely, if ever, leads to global unfolding. On this basis pathways of progressive openings can be proposed.

Materials and methods

Exchange measurements

Uniformly ^{15}N -labeled recombinant bovine ACBP was produced and purified as described previously (Kragelund et al., 1993). The purity and the labeling of the protein were examined by ESI-MS. A fraction of N-terminal acetylated ACBP molecules (5%) was present in the preparation. Amide hydrogen exchange was performed in deuterium oxide (Merck, Darmstadt, Germany). Two sets of samples were used. In one set exchange was followed at selected pH values between pH 5.2 and pH 8.1 at a constant temperature of 298 K. For the second set exchange was followed at temperatures between 280 and 300 K. At each temperature, pH was

adjusted to give a constant $[OD^-]$ of $1.55 \times 10^{-8} \pm 3.98 \times 10^{-9}$ M (Glascoe & Long, 1960; Covington et al., 1966). At the applied pH- and temperature ranges, ACBP is known to maintain a native and folded structure. For each pH, samples of 1 to 2 mM ACBP in H_2O were adjusted to the desired pH and lyophilized several times. After the final lyophilization, the protein was dissolved in 600 μL 99.99% D_2O , readjusted to the desired pH at the relevant temperature and transferred to a precooled NMR tube. This was immediately placed in the spectrometer, which in advance had been tuned and calibrated using a similar sample. Acquisition of the first experiment was initiated when the wanted sample temperature was obtained. pH was measured at the relevant temperature on a combined electrode pH meter (Radiometer, Denmark). All pH measurements in D_2O are reported as direct meter readings. Samples of ACBP were recycled by unfolding in 6 M guanidinium chloride, refolded and desalting on a P6-DG column in a 0.1 M NH_4HCO_3 buffer, readjusted to the wanted pH and lyophilized. Series of two-dimensional $^{15}N-^1H$ HSQC spectra (Bodenhausen & Ruben, 1980) were recorded for the two sets of samples with 2,048 and 64 or 32 complex points, respectively, in the t_2 and t_1 dimensions. With eight transients per increment, the total acquisition time was 22 or 11 min. Residual water signal was attenuated by applying low-power irradiation on the water resonance between transients producing an almost equal intensity damping on all resonance lines. The spectra were zero-filled once in both dimensions and no weighing functions were applied. All spectra were recorded and processed according to the States-Time-Proportional-Phase-Incrementation (TPPI) scheme (Marion et al., 1989) and the spectral widths in 1H and ^{15}N dimensions were 12.62 and 36.22 ppm, respectively. All experiments were recorded on a Bruker AMX-600 spectrometer equipped with a triple resonance 5 mm probe. Recorded chemical shifts were measured using references to 3-(methylsilyl)-propionic- d_4 -acid and liquid ammonia, respectively. The NMR data were processed and analyzed using the programs MNMR and PRONTO (Kjær et al., 1991, 1994). The PRONTO software package was used for computerized integration of cross peak intensities, data management, and registration in databases. Assignments of 1H and ^{15}N resonances were obtained from previous work (Andersen & Poulsen, 1994). Direct measured peak integrals were used as a first input to the fitting routine MFIT, where peak volumes were fitted to a Lorentzian peak form, providing uncertainties to the integral measurements. Decay curves of peak integrals with time were fitted to an exponential three-parameter decay of the form

$$I(t) = I(\alpha) + I(0)\exp(-k_o t) \quad (4)$$

where $I(t)$ is the intensity at time t after addition of D_2O to the lyophilized protein, $I(0)$ is the cross peak intensity at time zero, $I(\alpha)$ is the final cross peak intensity included accounting for baseline distortions, and k_o is the observed exchange rate constant. For amides where complete exchange was not reached in the time of experiment $I(\alpha)$ was omitted from the fits. Values and standard deviations of $I(\alpha)$, $I(0)$, and k_o were obtained from nonlinear fits using the routine EXPFIT. The uncertainties obtained on peak integrals were included in the fitting procedure. The time t of the recording was measured from the time of mixing to the time in the middle of the NMR data acquisition. Despite the dispersion of resonances in both the 1H and ^{15}N dimensions, the recording of certain exchange reactions was hampered. For the study of the pH

dependence, rate constants of hydrogen exchange in ACBP were measured for 56 amides.

Nonlinear fitting to obtain $k_1(i)$ and $k_2(i)$

The site (i) specific rate constants $k_1(i)$ and $k_2(i)$ of the pre-exchange equilibrium in Equation 1 were determined for amides of the EX(1/2) group using a set of nonlinear fitting routines of the pH dependence of the experimentally determined k_o . Three types of nonlinear fitting of experimental data to Equation 3 were performed. In one procedure the pH dependence of $k_o(i)$ was fitted in a three parameter fit to obtain $k_1(i)$, $k_2(i)$, and $k_3(i)$ assuming only that the opening and closing rate constants, $k_1(i)$ and $k_2(i)$, are independent of pH. In this case, consistent $k_1(i)$ values could be determined for most of the amides in the EX(1/2) group, however, $k_2(i)$ and $k_3(i)$, which are inversely correlated, could not be determined. In a second procedure, a nonlinear two-parameter fit of $k_1(i)$ and $k_2(i)$ to the pH dependence of $k_o(i)$ was used applying the calculated intrinsic rate constants, $k_3(I)$ (Bai et al., 1993), and assuming that the opening and closing rate constants, $k_1(i)$ and $k_2(i)$, are independent of pH. As seen in Equation 3, the two rate constants $k_1(i)$ and $k_2(i)$ are the only unknowns, when $k_o(i)$ and $k_3(i)$ are both known. Therefore, from a set of measured $k_o(i)$ values obtained at several pH values, and the known intrinsic $k_3(i)$ at each pH, $k_1(i)$ and $k_2(i)$ for the individual amides were obtained by nonlinear fitting to Equation 3. In a third procedure, a nonlinear one-parameter fit was used with an input of the known $k_1(i)$ from the first procedure and $k_3(i)$ to determine $k_2(i)$. In this fitting procedure, the uncertainty of $k_2(i)$ was determined from fitting with both the maximum and minimum values of $k_1(i)$ determined in the nonlinear three-parameter fit. The combination of the first and third procedure gave results very similar to those obtained by the second procedure. For amides in the EX2 group $k_1(i)/k_2(i)$ was determined from EX2 fits as described by Hvilstad and Nielsen (1966).

Energies of activation

From the temperature dependence of the observed exchange rates, the energies of activation for exchange, E_a^{HX} , were determined from an Arrhenius plot analysis. The amide exchange rates were measured at seven pH values in a 20° temperature range at non-denaturing temperatures.

Acknowledgments

We thank C. Rischel for assistance with the Levenburg–Marquardt fitting and P. Skovgaard and E. Knudsen for skilled technical assistance. This paper is a contribution from the Danish Protein Engineering Research Center, which was supported jointly by the Science Research Councils of Denmark.

References

- Andersen KV, Poulsen FM. 1993. Three-dimensional structure in solution of acyl-coenzyme A binding protein from bovine liver. *J Mol Biol* 226:1131–1141.
- Andersen KV, Poulsen FM. 1994. Refinement of the three-dimensional structure of acyl-coenzyme A binding protein using heteronuclear and three-dimensional n.m.r. spectroscopy. *J Biomol NMR* 3:271–284.
- Arrington CB, Robertson AD. 1997. Microsecond protein folding kinetics from native-state hydrogen exchange. *Biochemistry* 36:8686–8691.
- Bai Y, Milne JS, Mayne L, Englander SW. 1993. Primary structure effects on peptide group hydrogen exchange. *Proteins Struct Funct Genet* 17:75–86.

- Bai Y, Sosnick TR, Mayne L, Englander SW. 1995. Protein folding intermediates: Native-state hydrogen exchange. *Science* 269:192–197.
- Barksdale AD, Rosenberg A. 1982. Acquisition and interpretation of hydrogen exchange data from peptides, polymers and proteins. In: Glick D, ed. *Methods of biochemical analysis*, Vol. 28. New York: John Wiley & Sons. pp 1–113.
- Bodenhausen G, Ruben DJ. 1980. Natural abundance nitrogen-15 NMR enhances heteronuclear spectroscopy. *Chem Phys Lett* 69:185–189.
- Clarke J, Fersht AR. 1996. An evaluation of the use of hydrogen exchange at equilibrium to probe intermediates on the protein folding pathway. *Fold Design* 1:243–254.
- Covington AK, Robinson RA, Bates RG. 1966. The ionization constant of deuterium oxide from 5° to 50°. *J Chem Phys* 70:3820–3824.
- Englander SW. 1975. Measurement of structural and free energy changes in haemoglobin by hydrogen exchange methods. *Annu NY Acad Sci* 244:10–27.
- Englander SW, Downer NW, Teitelbaum H. 1972. Hydrogen exchange. *Annu Rev Biochem* 41:903–924.
- Frost AA, Pearson RG. 1953. *Kinetics and mechanisms*. New York: John Wiley & Sons. pp 160–164.
- Glascoe PK, Long FA. 1960. Use of glass electrodes to measure acidities in deuterium oxide. *J Phys Chem* 64:188–191.
- Gregory RB, Crabo L, Percy AJ, Rosenberg A. 1983. Water catalysis of peptide hydrogen isotope exchange. *Biochemistry* 22:910–917.
- Hvidt A. 1964. A discussion of the pH dependence of the hydrogen-deuterium exchange of proteins. *CR Trav Lab Carlsberg* 34:299–317.
- Hvidt A. 1973. Isotope hydrogen exchange in solutions of biological macromolecules. In: Sadron C, ed. *Dynamic aspects of conformation changes in biological macromolecules*. Holland: Reidel and Dordrect. pp 103–115.
- Hvidt A, Nielsen SO. 1966. Hydrogen exchange in proteins. *Adv Protein Chem* 21:287–386.
- Kim KS, Fuchs J, Woodward CK. 1993. Hydrogen exchange identifies native-state motional domains important in protein folding. *Biochemistry* 32:9600–9608.
- Kim KS, Woodward CK. 1993. Protein internal flexibility and global stability: Effects of urea on hydrogen exchange rates of bovine pancreatic trypsin inhibitor. *Biochemistry* 32:9609–9613.
- Kjær M, Andersen KV, Ludvigsen S, Shen H, Windekilde D, Sørensen B, Poulsen FM. 1991. Outline of a computer program for analysis of protein NMR spectra. Computational aspects of the study of biological macromolecules by nuclear magnetic resonance spectroscopy. In: Hoch JC, Redfield C, Poulsen FM, eds. *NATO ASI*, Vol. 225. pp 291–302.
- Kjær M, Andersen KV, Poulsen FM. 1994. Automated and semiautomated analysis of homo- and heteronuclear multidimensional nuclear magnetic resonance spectra of proteins: The program Pronto. *Methods Enzymol* 239:288–307.
- Kragelund BB, Andersen KV, Madsen JC, Knudsen J, Poulsen FM. 1993. Three-dimensional structure of the complex between acyl-coenzyme A binding protein and palmitoyl-coenzyme A. *J Mol Biol* 230:1260–1277.
- Kragelund BB, Højrup P, Jensen MS, Schjerling CK, Juul E, Knudsen J, Poulsen FM. 1996. Fast and one-step folding of closely and distantly related homologous proteins of a four-helix bundle family. *J Mol Biol* 256:187–200.
- Kragelund BB, Knudsen J, Poulsen FM. 1995a. Local perturbations by ligand binding of hydrogen deuterium exchange kinetics in a four helix bundle protein, acyl coenzyme A binding protein. *J Mol Biol* 250:695–705.
- Kragelund BB, Robinson CV, Knudsen J, Dobson CM, Poulsen FM. 1995b. Folding of a four-helix bundle: Studies of acyl-coenzyme A binding protein. *Biochemistry* 34:7217–7224.
- Linderstrøm-Lang K. 1955. Deuterium exchange between peptides and water. *Chem Soc Spec Publ* 2:1–20.
- Marion D, Ikura M, Tschudin R, Bax A. 1989. Rapid recording of 2D NMR spectra without phase cycling. Application to the study of hydration exchange in proteins. *J Magn Reson* 85:393–399.
- Mayo SL, Baldwin RL. 1993. Guanidinium chloride induction of partial unfolding in amide proton exchange in RNase A. *Science* 262:873–876.
- Mikkelsen J, Højrup P, Nielsen PF, Roepstorff P, Knudsen J. 1987. Amino acid sequence of acyl-coenzyme A binding protein from cow liver. *Biochem J* 245:857–861.
- Pedersen TG, Thomsen NK, Andersen KV, Madsen JC, Poulsen FM. 1993. Determination of the rate constants k_1 and k_2 of the Linderstrøm-Lang model for protein amide hydrogen exchange. *J Mol Biol* 230:651–660.
- Perrin CL. 1989. Proton exchange in amides: Surprises from simple systems. *Acc Chem Res* 22:268–275.
- Richards FM. 1979. Packing effects, cavities, volume fluctuations, and access to the interior of proteins. Including some general comments on surface area and protein structure. *Carlsberg Res Commun* 44:47–63.
- Rischel C, Andersen KV, Madsen JC, Poulsen FM. 1994. Comparison of backbone dynamics of apo and holo-acyl-coenzyme A binding protein using ^{15}N -relaxation measurements. *Biochemistry* 33:13997–14002.
- Roder H, Wagner G, Wüthrich K. 1985. Amide proton exchange in proteins by EX1 kinetics: Studies of the basic pancreatic inhibitor at variable p^2H and temperature. *Biochemistry* 24:7396–7407.
- Wagner G. 1982. Characterization of the distribution of internal motion in BPTI using a large number of internal NMR probes. *Quart Rev Biophys* 16:1–87.
- Wagner G, Wüthrich K. 1979. Structural interpretation of the amide proton exchange in the basic pancreatic trypsin inhibitor and related proteins. *J Mol Biol* 134:75–94.
- Woodward CK, Hilton BD. 1979. Hydrogen exchange kinetics and internal motions in proteins and nucleic acids. *Annu Rev Biophys Bioeng* 8:99–127.
- Woodward CK, Simon I, Thchsen E. 1982. Hydrogen exchange and the dynamic structure of proteins. *Mol Cell Biochem* 48:135–160.